PERGAMON

Atmospheric Environment 33 (1999) 2789–2806

ATMOSPHERIC ENVIRONMENT

Isotopic and molecular fractionation in combustion; three routes to molecular marker validation, including direct molecular 'dating' (GC/AMS)[1]

L.A. Currie[a,*], G.A. Klouda[a], B.A. Benner, Jr.[a], K. Garrity[a], T.I. Eglinton[b]

[a]*Chemical Science and Technology Laboratory, National Institute of Standards and Technology (NIST), Gaithersburg, MD 20899, USA*
[b]*Department of Marine Chemistry and Geochemistry, Woods Hole Oceanographic Institution, Woods Hole, MA 02543, USA*

Abstract

The identification of unique isotopic, elemental, and molecular markers for sources of combustion aerosol has growing practical importance because of the potential effects of fine particle aerosol on health, visibility and global climate. It is urgent, therefore, that substantial efforts be directed toward the validation of assumptions involving the use of such tracers for source apportionment. We describe here three independent routes toward carbonaceous aerosol molecular marker identification and validation: (1) tracer regression and multivariate statistical techniques applied to field measurements of mixed source, carbonaceous aerosols; (2) a new development in aerosol ^{14}C metrology: direct, pure compound accelerator mass spectrometry (AMS) by off-line GC/AMS ('molecular dating'); and (3) direct observation of isotopic and molecular source emissions during controlled laboratory combustion of specific fuels. Findings from the combined studies include: independent support for benzo(*ghi*)perylene as a motor vehicle tracer from the first (statistical) and second (direct 'dating') studies; a new indication, from the third (controlled combustion) study, of a relation between ^{13}C isotopic fractionation and PAH molecular fractionation, also linked with fuel and stage of combustion; and quantitative data showing the influence of *both* fuel type and combustion conditions on the yields of such species as elemental carbon and PAH, reinforcing the importance of exercising caution when applying presumed conservative elemental or organic tracers to fossil or biomass burning field data as in the first study. Published by Elsevier Science Ltd.

Keywords: Combustion aerosol; Carbon isotopic tracers; Elemental carbon; PAH; Isotopic and molecular fractionation; Stages of combustion; GC/AMS; Model validation; Biomass burning

1. Introduction

The identification of sources of combustion particles and their apportionment in environmental samples is of increasing importance, as the potential effects of such particles on human health, visibility, and climate become more widely recognized (Penner and Novakov, 1996). One special focus of carbonaceous aerosol studies, having spatial scales ranging from local (urban) to hemispheric or even global, is to discriminate quantitatively between anthropogenic (controllable) and natural source contributions (Buffle and van Leeuwen, 1992). A second, is to develop the historical record of carbonaceous

*Corresponding author. Tel.: 301 975 3919; fax: 301 216 1134; e-mail: lloyd.currie@nist.gov.

[1]Contribution of the National Institute of Standards and Technology; not subject to copyright.

1352-2310/99/$ - see front matter Published by Elsevier Science Ltd.
PII: S1352-2310(98)00325-2

aerosol emissions as found in ice cores, high altitude glaciers, and lacustrine and marine sediments (Cachier et al., 1997; Currie et al., 1998a; Masclet and Hoyau, 1994).

The 'ideal' that is often sought for accomplishing such goals is a unique, quantitative 'marker' or tracer for every significant, contributing source. That ideal has been approached through the use of morphological characterization (Goldberg, 1985), and the measurement of selected elements (Friedlander, 1973; Gordon, 1988); stable and cosmogenic carbon isotopes (Cachier, 1989; Currie et al., 1984), oxygen, sulfur, and lead (Sturges and Barrie, 1987) isotopes; and organic compounds (Rogge et al., 1993) emitted in the combustion process. In cases where a single substance marker is not unique to a given source, elemental or molecular *patterns* may provide the requisite specificity. In cases where markers are unique, but not absolute, statistical methods involving simple and multiple regression can generate the necessary calibration factors (Hopke, 1985).

A problem is that the presumed 'ideal' is not always achieved, or adequately validated, such that apportionment results are of uncertain quality or even totally misleading (Buffle and van Leeuwen, 1992, Chapter 1). That leads to the focus of the work reported here, which illustrates the identification and validation of selected isotopic, elemental, and molecular (organic) markers for sources of carbonaceous aerosols. The work involves three complementary routes to marker validation, including: (1) the measurement of selected presumed source tracers in a special ambient aerosol study, (2) direct carbon isotopic characterization of individual organic substances isolated from a carbonaceous aerosol reference material, and (3) the determination of molecular and isotopic fractionation patterns resulting from controlled, laboratory combustions reflecting a range of fuels and combustion conditions. We shall see that information derived from these three routes is complementary and supportive, with multivariate statistical implications from the field study being verified by independent direct 'molecular dating' of individual PAH in the second study, and by fuel and burn stage dependencies in the third, laboratory combustion study. In fact, the second and third studies shed some important scientific light on 'surprises' that arose in the first, atmospheric field study. The third study, in turn, generated its own surprises with respect to isotopic fractionation in the combustion process, and field-laboratory differences in certain pyrolysis products.

Only a brief review will be given of pertinent findings from the urban and atmospheric reference material (published) experiments, in Sections 2 and 3 of this paper, respectively; methods and results of the (unpublished) laboratory combustion study will be presented in more detail, in Section 4, with emphasis on the tracer validation links to the other studies.

2. Urban field study: isotopic, elemental, organic markers (Currie et al., 1994)

2.1. Setting and objectives

Wintertime sampling of ambient aerosol in Albuquerque, NM, provided an excellent means to evaluate alternative tracers for discriminating carbonaceous aerosol from wood burning and motor vehicle exhaust. Since the aerosol derived primarily from a single fossil and a single biomass source, ^{14}C was most appropriate for the quantitative apportionment of the carbon arising from each. This isotope was used in turn to assess (1) the potassium-lead multiple regression apportionment model, and (2) polycyclic aromatic hydrocarbon (PAH) tracers for the two source classes. An intercomparison of the three classes of carbonaceous aerosol tracers, based on ambient samples collected in Albuquerque, provided an important consistency check of validity.

The *multiple regression (MR) model* is based on the premise that the aerosol carbon can be partitioned by two unique regressors: mineral-corrected K, for the woodburning component, and Pb, for the motor vehicle component (Lewis and Einfeld, 1985). Calibration factors (regression coefficients) are derived by fitting the model,

$$C = b_0 + b_K \mathrm{K} + b_{Pb}\,\mathrm{Pb} + e \tag{1}$$

where the left side of the equation represents total aerosol carbon, and the second and third terms on the right represent wood carbon (WC) and fossil carbon (FC) aerosol, respectively; the symbol e represents the random error term. The first term, intercept b_0, should be zero if the two elemental tracers account for all of the aerosol carbon.

The *^{14}C model* provides a direct measure of WC, based on the $^{14}C/^{12}C$ ratio of the wood burned (approximately 'modern' – see Currie et al. [1984]) and the aerosol carbon mass, with FC representing the remainder of the aerosol carbon mass. WC and FC derived from this model can then be used to provide an independent check on the MR coefficients for K and Pb by using simple regression:

$$\mathrm{WC} = b_0 + b_K \mathrm{K} + e \tag{2a}$$

$$\mathrm{FC} = b_0' + b_{Pb}\,\mathrm{Pb} + e \tag{2b}$$

where, as with Eq. (1) the intercept terms should be zero if the potassium and lead tracers satisfactorily account for the wood and fossil aerosol carbon, respectively.

The *multivariate model* is based on principal component analysis of the elemental data together with a suite of PAH ranging from phenanthrene to coronene, and including the conifer (abietane) pyrolysis products, retene and the methyl ester of its precursor dehydroabietic acid.

2.2. Principal outcomes, and surprises

The MR model failed to fit the entire dataset. Even with a non-zero intercept, Eq. (1) could not be fit to a plane. A negligible intercept and satisfactory fit was obtained for daytime samples, however, but those samples collected at night gave a significantly non-zero intercept. With a value of 10.5 $\mu g\,m^{-3}$, the intercept represented about one-third of the total nighttime aerosol carbon. Also, the difference between the observed aerosol carbon at night and that predicted by the daytime elemental tracer (K, Pb) model showed a nighttime excess of 14% to 69% (interquartile range).

Based on a comparison of the K-coefficient and ^{14}C and the simple regressions of Eqs. (2), the excess carbon was found to be associated with woodburning. The simple regression with Pb showed a good fit, with a negligible intercept. The multivariate model showed an anticorrelation between temperature and softwood pyrolysis products, such as methyl dehydroabietic acid (*mdha*), and a strong positive correlation between the motor vehicle tracer, Pb, and the PAH benzo(*ghi*)perylene (b(*ghi*)p).

These findings are summarized in Fig. 1, which displays the first two principal components, representing 92% of the variance, for five variates and twelve samples. The approximately linear path for the daytime samples (D) between K and Pb reflects the adequacy of the elemental tracer model during the day, whereas the displacement of the nighttime samples (N) away from this path, toward the softwood pyrolysis product *mdha* reflects the excess (intercept) carbonaceous aerosol at night. We conclude that the nature of the woodburning emissions is significantly affected by the combustion conditions, as reflected by day/night differences and air temperature. The other conclusion from the study, as evidenced in Fig. 1, is that b(*ghi*)p appears to be a tracer for carbonaceous aerosol emissions from motor vehicles, because of its strong association with lead. This latter finding holds special interest for carbonaceous aerosol from motor vehicles, because of the phasing out of Pb tetraethyl as a fuel additive.

3. Molecular 'dating' study; direct isotopic measurement of individual PAH (Currie et al., 1997)

3.1. Objectives: molecular marker validation; source apportionment at the molecular (individual compound) level

Multivariate statistical evidence for elemental source tracers or organic molecular (source) markers, such as that given above for b(*ghi*)p has become widely relied upon both for the development of molecular source 'fingerprints' and for the subsequent quantitative apportionment of aerosol source contributions at a receptor site. Just as statistical association does not necessarily imply causation, however, multivariate factor and clustering techniques cannot be taken as proof of a molecular marker – source connection. Pitfalls abound (Currie, Chapter 1 in Buffle and van Leeuwen, 1992]. One means for validating suggested relationships are direct emissions experiments on individual combustion sources, similar to the laboratory combustion study that comprises the third part (Section 4) of this paper. A less common alternative can be employed *when the presumed molecular markers themselves contain unique tracer isotopes*, such as the biomass burning tracer ^{14}C. In effect, one can achieve direct (non-statistical) molecular marker validation by measuring tracer isotopes *in* the presumed tracer compound. This approach has the special advantage of testing the source–tracer relationship *at the receptor site*. It is thus relatively immune to transformations in tracer amounts or tracer patterns that may occur between the source and receptor locations. Like Chemical Mass Balance, this method can be applied to individual or composite samples; in contrast to multiple regression or factor analysis, results from an array of samples (data matrix) are not required. *Methodologically, this work represents the first application of the new technique of GC/AMS to an atmospheric sample*, in this case an SRM. Although performed off-line, the study demonstrates the great importance of individual compound 'dating' in environmental samples, since such samples will invariably represent mixed sources and may therefore be isotopically heterogeneous at the molecular level.

3.2. Approach

The method employed for developing or validating carbonaceous aerosol molecular markers was based on the measurement of the ^{14}C isotopic abundance in pure fractions of the isolated molecular species, using off-line gas chromatography/accelerator mass spectrometry (GC/AMS) (Eglinton et al., 1996). The first test and application of GC/AMS to atmospheric aerosol was performed using an NIST urban particle Standard Reference Material (SRM) 1649a (Currie et al., 1997). This material was sampled in large quantity in Washington, DC, for the purpose of preparing bulk amounts of urban atmospheric particulate matter, certified for trace organic compounds, especially PAH (NIST, 1998). Steps employed for the GC/AMS experiment consisted of organic extraction with dichloromethane, followed by liquid chromatographic separation of the aromatic fraction, isolation of individual PAH using preparative scale capillary gas chromatography (PCGC), and measurement of ^{14}C in the isolated compounds by accelerator mass spectrometry. Although the technique is reliable and reasonably straightforward, it will not immediately become

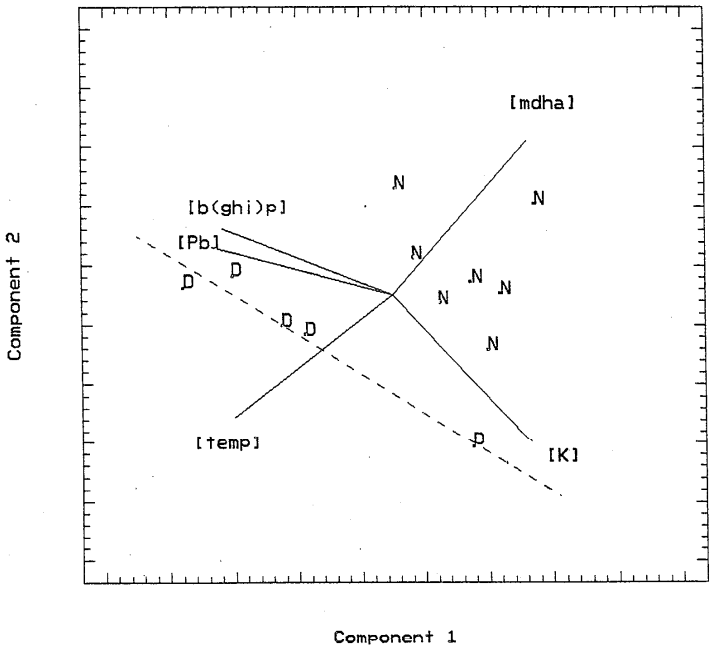

Fig. 1. Planar principal component (PC) projection from 5-variate space, representing Albuquerque air temperature and carbon-normalized elemental and organic data for day ('D') and night ('N') aerosol samples. Unique tracers and implied end member sources are: K, woodburning carbon (flaming stage); methyl dehydroabietic acid (mdha), woodburning (smoldering stage); Pb, motor vehicle carbon. Strong associations: mdha, temperature (negative correlation); Pb, benzo[*ghi*]perylene [b(*ghi*)p, positive correlation). The 'D' samples are consistent with a one dimensional (2-source) mixing line (dashed), but the 'N' samples show additional anticorrelation with temperature. PC's 1 and 2 capture 92% of the 5-space variance. [Adapted from Currie et al. (1994).]

a field method for PAH in atmospheric aerosol because AMS requires at least tens of micrograms for each compound measured, and individual PAH are found at relatively low levels, typically 0.1–10 $\mu g\,g^{-1}$ in atmospheric aerosol.

GC/AMS applied to potential molecular markers for fossil or biomass combustion aerosol in effect yields fossil-biomass apportionment at the molecular level. A presumed unique fossil tracer, such as b(*ghi*)p, should contain no ^{14}C, while a unique biomass combustion tracer, such as retene, should contain the $^{14}C/^{12}C$ ratio characteristic of the living biosphere. Between these extremes, the ^{14}C content will give the portion of non-unique organic tracers arising from each of the two (source) end members. It is clear that the application of GC/AMS to a set of non-unique tracers could be used to generate source profiles, or molecular marker patterns. Using ^{14}C to measure the fraction of fossil carbon $f_{FC}(i)$ in a series of individual (PAH) compounds with concentrations PAH(i), the resulting PAH molecular marker pattern for fossil carbon would be given by $f_{FC}(i)\,\mathrm{PAH}(i)$. Similarly, the biomass carbon PAH molecular marker pattern would be $(1-f_{FC}(i))\,\mathrm{PAH}(i)$. If the sample came from an airshed having a single fossil and a single biomass carbonaceous aerosol source, the molecular marker patterns would reflect those of the two sources, *at the receptor site, for the particular sample analyzed.* If two or more biomass and fossil mass sources were involved, the derived patterns would represent appropriately weighted averages for each (bio-, fossil-) source class. By subjecting a series of samples to the technique, one would gain the enormous advantage of learning about source profile variability (including covariance) at the receptor site. This *cannot be achieved* by multivariate statistical methods as commonly practiced.

3.3. Results

Like the array of atmospheric samples collected in the Albuquerque study, the (SRM 1649a) reference material collected in Washington, DC, represented a mixture of fossil and biomass sources, with an average fossil carbon contribution of ca. 57% (Currie et al., 1984). This earlier result, together with that for the aromatic fraction of the particles (88% fossil), already showed dramatic isotopic heterogeneity, reflecting mixed sources having different molecular emissions profiles. GC/AMS now makes it possible to extend ^{14}C characterization to individual

trace compounds such as the twenty-four certified PAH in SRM 1649a, having concentrations ranging from ca. 0.15 mg kg^{-1} (dibenz[*a,h*]anthracene) to ca. 6.5 mg kg^{-1} (fluoranthene) (NIST, 1998).

Following extraction and separation of polar and non-polar fractions of SRM 1649a, individual fractions of six PAH were isolated using 102 cycles of automated PCGC. A stacked chromatogram (FID) of the six PCGC-separated fractions is given in Fig. 2, together with the residue in the seventh, 'waste trap.' AMS was then performed on the individual PAH fractions to determine the relative fossil-biomass contribution to each. The combined ^{14}C data for the Urban Particle SRM, including results for as little as 35 μg of individual PAH, are given in Table 1. The contrast between polar and aliphatic and molecular (PAH) fractions is striking, confirming the vast chemical differences in fossil-biomass source impacts. The result for benzo(*ghi*)perylene is of special interest in light of the prior statistical implications of the Albuquerque study. It is confirmed by the direct ^{14}C assay as a largely fossil source tracer in this urban setting. The uncertainty interval, 83–100% fossil results primarily from the portion of the 'unresolved complex mixture' (*ucm*) co-collected in the benzo(*ghi*)perylene

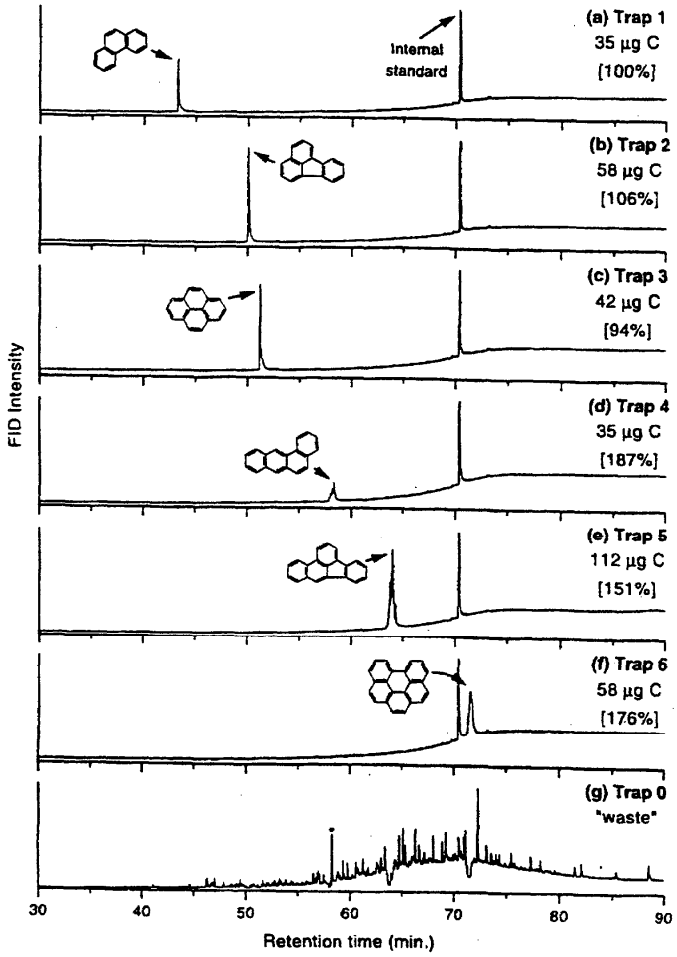

Fig. 2. Partial HRGC (FID) traces of PCGC-isolated fractions from SRM 1649a. See Fig. 5a in Currie et al. (1997) for details of instrument and column configuration. The GC oven was temperature programmed from 40°C (1 min. hold) to 320°C (20 min. at final temp.) at 4°C min^{-1}. Individual compound traps are (a) phenanthrene, (b) fluoranthene, (c) pyrene, (d) benz[*a*]anthracene, (e) benzofluoranthenes, (f) benzo[*ghi*]perylene. Trap 0 (g) contains the accumulated products of the sample remaining after isolation of the compounds of interest. An internal standard (terphenyl-d14) was added to the compound traps for quantitation purposes. Yields (as μg C) and trapping efficiencies (relative to phenanthrene) are shown. [Reprinted from Currie et al. (1997).]

Table 1
AMS (^{14}C) results for SRM 1649 (urban particles)[a]

Fraction	Mass-C μg	Modern-C[c] (%)	Fossil-C[c] (%)
Total carbon[b]	—	61	57
Aliphatic carbon	765	2.4	98
Polar carbon	984	43	70
Aromatic carbon[b]	—	17	88
Compound [PAH]			
1. Phenanthrene	35	—[d]	—[d]
2. Fluoranthene	58	20	86
3. Pyrene	42	—[d]	—[d]
4. Benz[*a*]anthracene	35	12	92
5. Benzofluoranthenes	112	15	89
6. Benzo[*ghi*]perylene	58	14	90

[a] Adapted from Currie et al. (1997 Table 4).
[b] Currie et al. (1984).
[c] Measurement uncertainties (Poisson-σ's) for the decay counting data of Currie et al. (1984) are about 4% modern carbon. For the other (AMS) data shown here, they range from 0.3 to 0.6% modern carbon. Modern carbon is defined by reference to the radiocarbon dating standard (SRM 4990B); fossil carbon is derived from this by taking into account the effect of atmospheric nuclear testing on the ^{14}C content of the living biosphere at the time of sampling (1973).
[d] No data because of poorly performing graphite AMS target.

trap. Improved pre-purification techniques of the aromatic fraction have since been applied, using silica gel flash chromatography and HPLC PAH ring size fractionation with an aminosilane column (Wise et al., 1977). This scheme has successfully removed *ucm* from the heavier PAH fractions yielding baseline resolved PAH ranging from chrysene to benzo(*ghi*)perylene from NIST sediment SRMs 1941a and 1944 (Pearson et al., 1997). Work is underway to apply the improved methodology to the atmospheric particulate SRM 1649a, to reduce the fossil carbon uncertainty to the AMS measurement imprecision (relative standard uncertainty) of ca. 1% or less. (See note added in proof.)

4. Laboratory combustion study of isotopic-molecular fractionation

Closing the loop between the varying composition of combustion aerosol in ambient samples, and the isotopic composition of individual substances and chemical fractions, is the direct observation of isotopic and molecular fractionation during the combustion of known source materials. This study was undertaken to look for the possibility of carbon isotopic fractionation in combustion aerosol, and the link to organic carbon emissions as a function of source material (fuel) and combustion stage. The possibility of isotopic fractionation must be considered because of the incomplete combustion, that is reflected, for example, in the observation of CO and carbonaceous aerosol as reaction products. Since natural source fuels are essentially fossil or biomass, with the exception of peat, and because isotope effects are generally small, the carbon isotope of interest in this study is stable ^{13}C, which has a natural abundance of ca. 1%.

4.1. ^{13}C as a combustion source tracer, and modes of isotopic fractionation

Like ^{14}C, ^{13}C can be useful for combustion source identification, as a result of small, but distinctive variations linked primarily with photosynthetic cycles or fossil fuel maturation processes. The 'C3' plants, which include most temperate zone trees and other vegetation, have relative $^{13}C/^{12}C$ values [$\delta^{13}C$] of ca. -25 per mil relative to the isotopic reference material 'VPDB', whereas 'C4' plants, which include tropical grasses, sugar cane, corn, etc., have $\delta^{13}C$ values of ca. -10 per mil.[2] Fossil fuels can cover a wide range from ca. -25 per mil to less than -40 per mil, depending on the nature of the fuel and its formation (Fritz and Fontes, 1980). To relate source $\delta^{13}C$ values to $\delta^{13}C$ in products of incomplete combustion, however, we must take into account possible combustion isotopic fractionation, which can be of two types. If the source material is chemically and isotopically homogeneous, then isotopic fractionation may arise from kinetic isotope effects. If not, the isotopic composition of products can also reflect differences in the internal fuel components (e.g., lignin, cellulose components of wood), and the relative distributions of combustion products from each of the internal components,

[2] The 'delta' notation that is widely used in stable isotope geochemistry is employed to indicate the relative deviation of an isotope ratio from an accepted isotopic standard. Quoting from Fritz and Fontes (1980), 'This relative difference is called the δ-value and [is] defined as

$$\delta x = (R_x - R_{std})/R_{std}$$

where R_x represents isotope ratios of a sample (... , $^{13}C/^{12}C$, $^{18}O/^{16}O$, ...) and R_{std} is the corresponding ratio in a standard. The δ-value is generally expressed in parts per thousand (permil, ‰), and written as

$$\delta x = ((R_x/R_{std}) - 1) \times 10^3.$$

A sample with a $\delta^{18}O = +10‰$ is thus enriched in ^{18}O by 10‰ (or 1%) relative to the standard. For ^{13}C, the accepted standard is 'VPDB' a limestone distributed by the International Atomic Energy Agency. Further information on light element stable isotope reference materials and accepted international guidelines for reporting stable isotope ratios may be found in Coplen, et al. (1996).

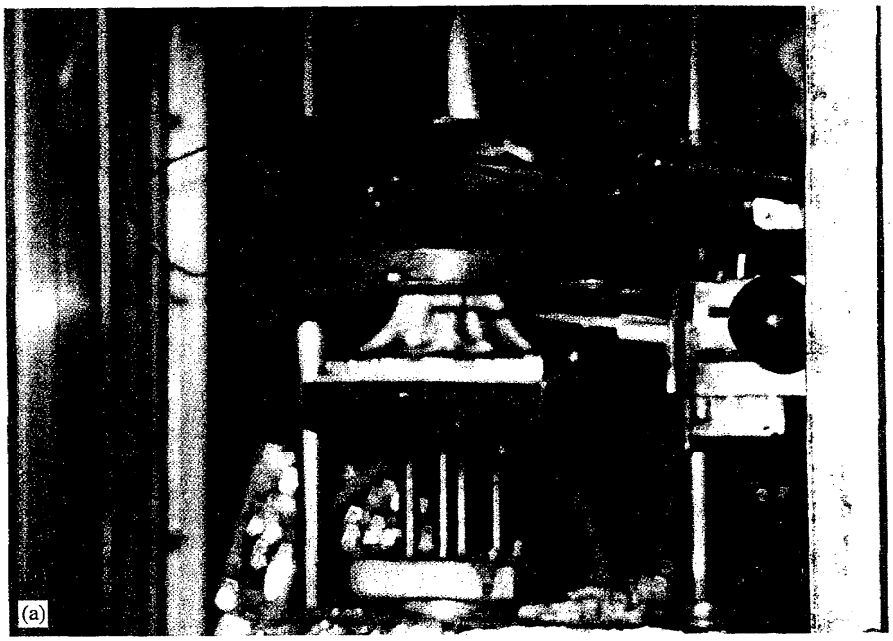

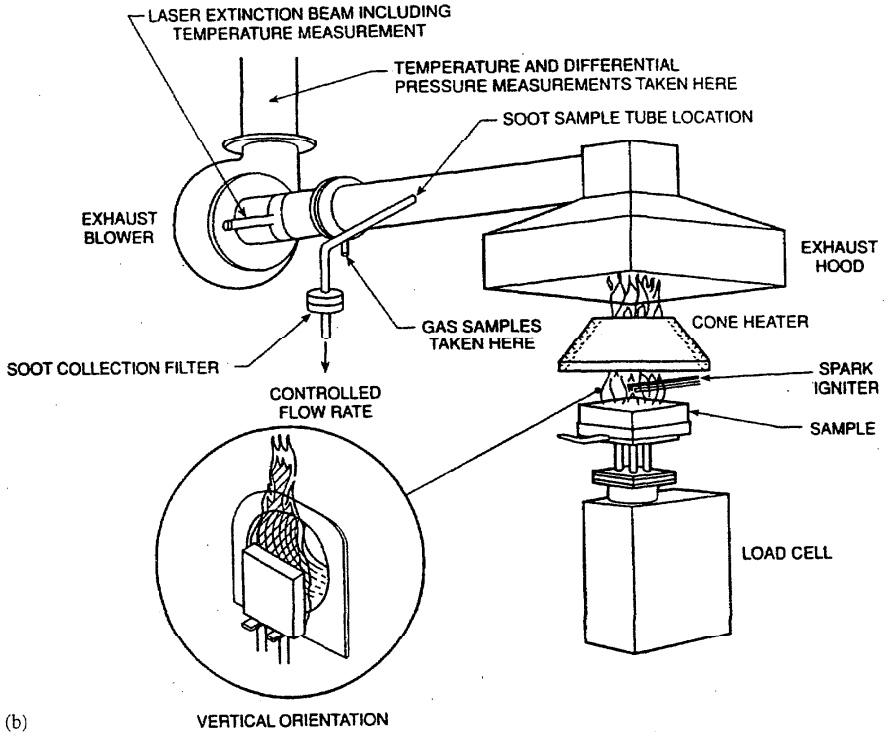

Fig. 3. Cone calorimeter. (a) Photograph showing the flaming stage combustion of one of the wood samples, supported by a stand on the load cell. Flame from the sample is visible both below and above the cone heater; gases and aerosols are swept by the convective air flow into the exhaust hood and sampling train. (b) Schematic diagram of the cone calorimeter system.

much like the superposition of emissions profiles from independent sources in the ambient atmosphere, with one important difference. The heterogeneous fuels can be characterized by relatively precise average compositions.

4.2. Design of the experiment

Controlled combustion experiments were performed in a laboratory of the NIST Fire Science Division, using the well-instrumented 'Cone Calorimeter,' depicted in Fig. 3 (Babrauskas, 1982). Source materials were placed on a 'load cell' which made it possible to monitor mass loss during the entire heating/combustion process. In addition to visual indications, the stage of combustion was quite apparent through distinctive rates of mass loss. Gaseous combustion products, notably CO and CO_2, were monitored also continuously during the process; and particulate carbon samples were taken at selected stages through the use of the 'soot collection filter.' Following the combustion process, CO and aerosol samples were returned to our laboratory for sample preparation for isotopic (^{13}C) and chemical analysis.

The experiment was designed to sample a range of fossil and biomass fuel classes, and to investigate chemical and isotopic effects as a function of burn stage and fuel type. The design also incorporated 'the rule of two' – i.e., two replicates for each cell in the design matrix. The columns of the design matrix were simply the combustion stages: smoldering, flaming, and glowing. The rows represented the source materials (fuels), which fell in two broad categories: biomass vegetation and fossil hydrocarbon fuels. Within these categories we had, BIOMASS: C3 plants (red oak, pinyon pine), C4 plants (cane leaves, dry/wet tripsicum grass); FOSSIL MASS (hydrocarbons): paraffin wax, butane gas. The current report is limited to results for the solid C3 and fossil hydrocarbon fuels. Material isolated by burn stage for isotopic (^{13}C) and/or chemical analysis includes CO and carbonaceous aerosol. The latter was to have been analyzed for (1) total carbon (TC) (and ^{13}C), (2) elemental carbon (EC) (and ^{13}C), (3) PAH, (4) selected trace elements, and (5) microparticles. Thus far, chemical data have been produced for (1)–(3), and isotopic (^{13}C) data for (1). Special instrumentation/techniques employed included: cone calorimetry, high precision isotope ratio mass spectrometry (^{13}C), thermal-optical EC analysis, and supercritical fluid extraction-gas chromatography/mass spectrometry (PAH).

4.3. Initial results for wood and hydrocarbon solid fuels

We report here combustion profiles plus isotopic and chemical data for two C3 wood fuels that are commonly used for fireplaces and wood stoves, oak and pinion pine, and a solid hydrocarbon fuel, paraffin wax. The pinion pine has a special link also to the Albuquerque field experiment summarized in the first part of this paper, for it constituted the major residential wood fuel at the time of that study. The wood fuels, of course, were heterogeneous both isotopically and chemically, with major cellulosic and lignin fractions, and the pine contained as well a major, volatile resinous component. Paraffin wax is less heterogeneous, but it does contain a mix of C_{20} to C_{24} normal alkanes (paraffin hydrocarbons) which comprise one of the highest boiling fractions (above 275°C) produced during the fractional distillation of petroleum. These particular fuels were selected to provide a contrast between wood and hydrocarbon source materials, as well as a contrast between two common but distinctive wood classes (deciduous, conifer). Solid fuels were selected for this initial study, to permit careful weighing and to take advantage of the special attributes of the Cone Calorimeter combustion system. Although all three fuels have ^{13}C compositions typical of the C3 class, they were significantly different in both their initial average $\delta^{13}C$ values, and in their isotopic fractionation behavior.

4.3.1. Combustion profiles

Combustion patterns were determined for duplicate specimens of each of the three fuel types by monitoring residual mass on the load cell as a function of time, as the fuels passed through three stages: initial smoldering, ignition and flaming combustion, and a final, glowing phase during which resulting char was gradually converted to CO and CO_2. Relative losses, normalized to the flaming stage, are shown in Fig. 4. Not surprisingly, all three fuels exhibited the maximum mass loss during flaming combustion, and oak and pine generated similar relative amounts of char (ca. 20%). Otherwise, interfuel differences were substantially greater than intrafuel (replicate sample) differences, with the paraffin wax having practically all of its mass consumed during the flaming stage.

Detailed mass loss rate profiles for the three pairs of samples are given in Fig. 5, and quantitative mass and chemical data are included in Table 2. The loss rate function, which serves as a measure of combustion intensity, was based on the smoothed (negative) first differences of the residual mass curve. Since the specimen masses were sampled at 5 s intervals, the smoothed data were divided by 5 to express loss rates as $g\,s^{-1}$.

A number of observations derive from the mass loss rate profiles. (1) The replicate pairs make clear the existence of characteristic fuel type differences, even between the two types of woods. (2) Major mass loss (and rate of mass loss) occurs during the flaming combustion stage, which is preceded by an initial smoldering stage, and followed by a final glowing stage. The wood samples are marked by an initial plateau with moderate mass loss, and by a final glowing stage with approximately exponentially declining residual sample mass. The wax samples also show minor initial and final segments but nearly

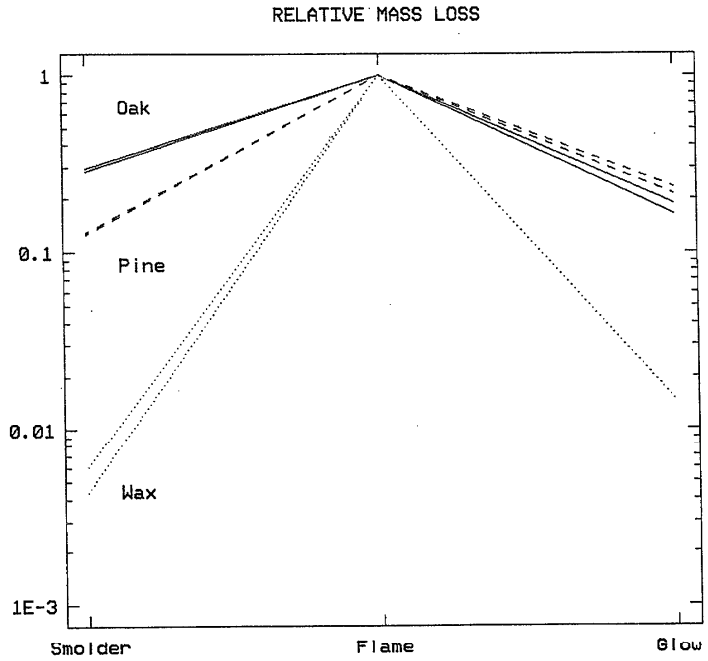

Fig. 4. Relative mass loss vs. combustion stage and fuel. Mass loss, relative to that for the flaming stage, is indicated for duplicate samples of oak (solid lines), pine (dashed lines) and paraffin wax (dotted lines). Differences among fuels far exceed intra-fuel variations. Smoldering (pre-ignition) stage mass loss for oak is more than twice that of pine, and negligible for wax. Glow or char (post-flaming) mass loss is also negligible for wax, but comparable for oak and pine. Note that maximum CO_2 production occurred during the flaming stage for all three fuel types; maximum CO production occurred also during flaming for the paraffin wax fuel, but during the char combustion (glowing) stage for the wood fuels.

all of the mass loss occurs during the flaming stage. (3) Several generalizations, related to parameter trends in passing from oak (O) to pine (P) to paraffin wax (W), follow from the profiles and the quantitative data tabulated in Table 2. (3a) Maximum combustion intensity (fuel consumption rate), which occurs near the end of the flaming stage, is sharper and ca. 50% higher for pine compared to oak, and sharper and higher still for wax. Similarly, the flaming mass loss fraction increases from 0.63 [O] to 0.70 [P] to 0.98 [W]. (3b) Smoldering plateaux become shorter and less intense [O > P > W]. The paraffin wax, in fact, exhibits no plateau, but rather a continually increasing loss rate, peaking just before extinction. (3c) The time constant for mass loss during the final (glowing) stage decreases by nearly a factor of two [O > P > W]. As shown in Fig. 4, the relative amount of material ('char') associated with this stage is quite significant for the wood specimens, but negligible ($\leq 1\%$) for the wax.

4.3.2. *Total carbon (TC), elemental carbon (EC), and pyrene*

The compositions of aerosol samples collected during the combustion process were also consistent with the trend among fuel types. Unlike the continually monitored profiles, samples collected during the three combustion stages were discrete and manual, with imperfect timing, especially for the smoldering stage. The times that filters were placed and replaced are indicated in the captions to Fig. 5, and it may be seen that first stage timing inconsistencies occurred for the wax samples, where Wax-1 had a larger admixture of material from the start of the flaming stage. Results nevertheless showed that absolute as well as relative amounts of carbon in the aerosol collected during flaming increased dramatically with the same trend [O < P < W], with essentially all of the flaming aerosol mass as carbon in the case of the wax. It is noteworthy that for all three fuels the smoldering stage carbonaceous aerosol was almost entirely organic: $99.1 \pm 0.3\%$ (oak), $98.4 \pm 1.3\%$ (pine), and $92.2 \pm 1.4\%$ (wax). (Means and standard uncertainties are shown.) In contrast, the flaming stage carbonaceous aerosol was primarily elemental, but with a somewhat greater dependence on fuel type: $86 \pm 2\%$ (oak), $90 \pm 3\%$ (pine), and $94 \pm 3\%$ (wax).

Masses are given also for pyrene, used as a surrogate for pyrogenic (pyrosynthetic) polycyclic aromatic hydrocarbons (PAH), since this PAH, like EC, is formed in

flaming combustion from all carbonaceous fuels. Amounts of (total) carbon and pyrene, given for smoldering and flaming stage aerosol samples, show that both absolute and relative amounts (pyrene/C) increase with fuel type [O < P < W], and that the relative mass of carbon (C/pyrene) is far greater in the smoldering stage, especially for the pine specimens. This reflects the fact that PAH tend to be formed during high temperature

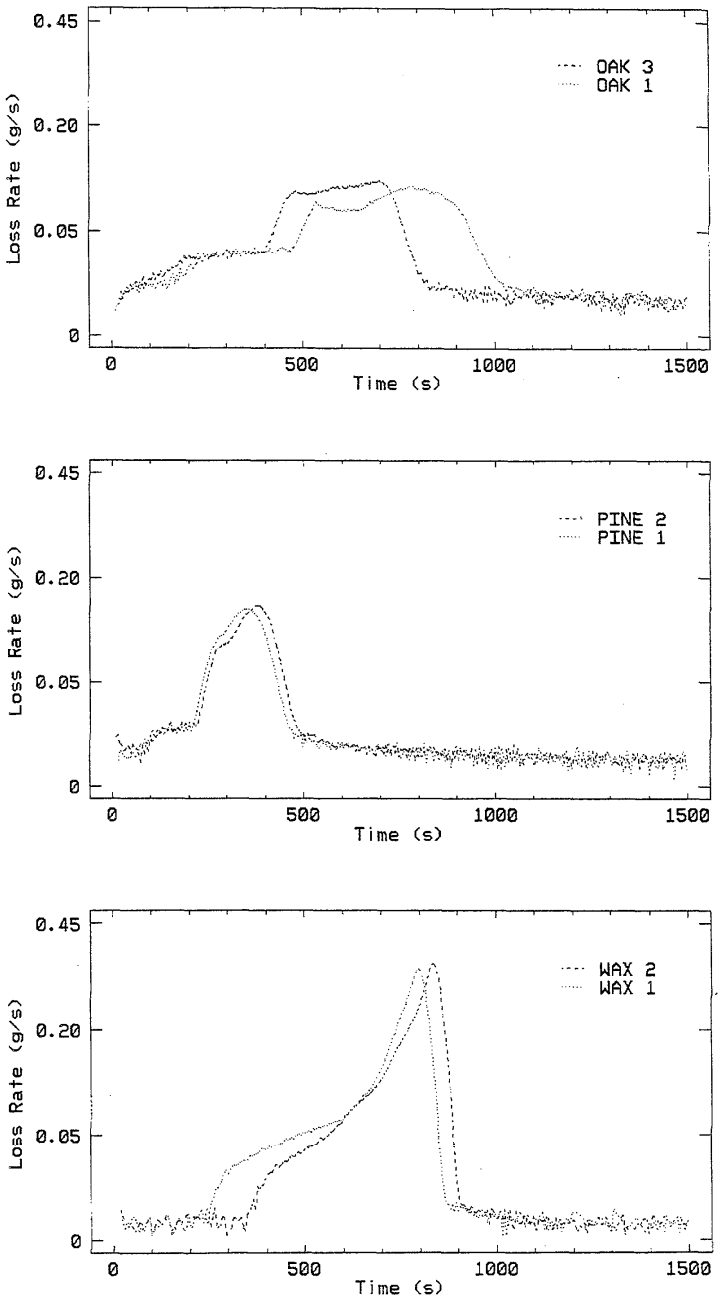

Fig. 5. (Caption on opposite page)

Table 2
Combustion characteristics (flaming stage)[a]

	Oak	Pine	Paraffin wax
Maximum loss rate ($g\,s^{-1}$)	0.107 ± 0.003	0.148 ± 0.003	0.337 ± 0.006
$\delta^{13}C$ (per mil)	-25.32 ± 0.08	-21.22 ± 0.06	-28.37 ± 0.13
Mass loss fraction	0.633 ± 0.002	0.698 ± 0.003	0.979 ± 0.002
Carbon (% of particle mass)	67 ± 8	78 ± 10	97 ± 5
Elemental carbon (% of C)	86 ± 2	90 ± 3	94 ± 3
Carbon/Pyrene ($\mu g\,ng^{-1}$)			
Smoldering stage	37	37	14
Flaming stage	4.9	3.5	2.5

[a] Uncertainties (±) represent standard errors (standard uncertainties) based on the differences between replicates.

pyrosynthesis processes, while carbon compounds may be formed also by lower temperature volatilization and degradation processes such as dehydrogenation (LaFlamme and Hites, 1978).

4.3.3. Isotopic composition

Table 2 shows that the ^{13}C compositions of carbonaceous aerosol formed during the flaming stages of the three fuels differ substantially, although all lie in the general range for C3 materials. The uncertainties of ca. 0.1 per mil are considerably smaller than those differences. At the same time the magnitude of the interfuel differences in the combustion aerosol suggests that the stable isotope of carbon may provide useful source discrimination, complementing that of ^{14}C. A major question that must first be addressed, however, is the extent to which isotopic fractionation occurs during incomplete combustion. This, in fact, was one of the main stimuli for this study.

To examine this question we first prepared replicate samples of the oak and pine source materials, and combusted them totally to CO_2, for stable isotope mass spectrometry. The results were startling. In contrast to the 0.1 per mil sample reproducibility seen with the flaming aerosol samples, and measurement reproducibility of ca. ten times better than that, we found differences of 0.9 per mil among triplicate samples of *both* wood source materials. Isotopic heterogeneity, resulting from chemical heterogeneity of the two types of wood, thus set a severe limitation to our ability to look for subtle isotope effects during combustion. The solution was to prepare homogeneous samples of the wood specimens to give a reliable measure of the average ^{13}C contents prior to combustion. This was accomplished by low-temperature ($-196°C$) pulverization, as developed for the National Biomonitoring Specimen Bank at NIST (Zeisler et al., 1983). The resulting samples are perhaps the first isotopically homogeneous wood Reference Materials [RMs]. Duplicate samples of these Oak and Pine RMs gave $\delta^{13}C$ values (per mil) of -24.55 and -24.55 [Oak], and -20.84 and -20.83 [Pine]. Measurements were then made of $\delta^{13}C$ in smoldering and flaming stage

Fig. 5. **Combustion loss rate profiles.** The rate of mass loss ($g\,s^{-1}$) as a measure of combustion intensity is shown as a function of time (s), using a square root transform to better display the structure at small loss rates. **(a) Oak fuel (top panel).** Aerosol samples were collected as follows: smoldering: oak-3 (135 s–422 s), oak-1 (50 s–497 s); flaming: oak-3 (422 s–849 s), oak-1 (497 s–1033 s); glowing (char combustion): oak-3 (849 s–1985 s), oak-1 (1033 s–2165 s). The time constant for the (exponential) mass loss during the glowing stage was 1290 ± 50 s (standard error based on difference between the two samples). Masses of aerosol-carbon (total carbon (TC), and elemental carbon (EC)) and pyrene recovered during the smoldering and flaming stages [sample oak-3], respectively, were: TC (364 μg, 334 μg); EC (2.9 μg, 287 μg); pyrene (9.9 ng, 68 ng). The aerosol deposit was negligible during the glowing (char) stage. **(b) Pine fuel (center panel).** Aerosol samples were collected as follows: smoldering: pine-1 (34 s–234 s), pine-2 (20 s–243 s); flaming: pine-1 (234 s–469 s), pine-2 (243 s–520 s); glowing (char combustion): pine-1 (469 s–1565 s), pine-2 (520 s–1625 s). The time constant for the (exponential) mass loss during the glowing stage was 920 ± 12 s (standard error based on difference between the two samples). Masses of aerosol-carbon and pyrene recovered during the smoldering and flaming stages [sample pine-2], respectively, were: TC (196 μg, 754 μg); EC (3.1 μg, 679 μg,); pyrene (5.3 ng, 220 ng). The aerosol deposit was negligible during the glowing stage. **(c) Paraffin wax fuel (bottom panel).** Aerosol samples were collected as follows: smoldering: wax-1 (114 s–259 s), wax-2 (108 s–373 s); flaming: wax-1 (259 s–940 s), wax-2 (373 s–954 s); glowing (char combustion): wax-1 (940 s–2090 s), wax-2 (954 s–2100 s). The time constant for the (exponential) mass loss during the glowing stage was 730 ± 150 s (standard error based on difference between the two samples). Masses of aerosol-carbon and pyrene recovered during the smoldering and flaming stages [sample wax-1], respectively, were: TC (109 μg, 3990 μg); EC (8.5 μg, 3630 μg); pyrene (7.6 ng, 1620 ng). The aerosol deposit was negligible during the glowing stage.

aerosol samples of all three solid fuels. Results are displayed in Fig. 6. This figure shows fuel dependent isotope effects, that generally are smaller or at most comparable to the wood fuel isotopic heterogeneity. The paraffin wax smolder-stage samples presented a special challenge, because of imperfect manual aerosol sample collection timing, and because of the enormous relative abundance of the flaming stage carbonaceous aerosol. Taking into account the difference in actual smoldering aerosol sampling times and the transition to the flaming stage as indicated by the trace in Fig. 5, we used an isotopic mass balance approach to make a modest correction (− 0.57 per mil) to the observed $\delta^{13}C$ value for sample Wax-1 (smoldering).

Average isotopic fractionation effects for the three fuels may be examined quantitatively, by calculating the $\delta^{13}C$ differences between the flaming stage aerosol and the fuels for each sample pair. Unfortunately, because of an experimental mishap, we did not obtain a $\delta^{13}C$ value for the particular lot of the hydrocarbon fuel combusted. Lacking this information for the hydrocarbon fuel, *per se*, the smoldering stage aerosol isotopic composition was used for the comparison; this may be reasonable, as 'smoldering' in this case is believed to be more of a distillation process than the more intensive oak and pine thermal decompositions reflected in the smoldering plateaux in Fig. 5a and b. (See also Fig. 7.) The parametric trend noted earlier is once again seen [O < P < W]. Isotopic differences ($\delta^{13}C$ [flame aerosol] − $\delta^{13}C$ [fuel]) and standard errors are: − 0.70 ± 0.08 per mil [OAK], − 0.39 ± 0.05 per mil [PINE], and + 1.26 ± 0.035 per mil [WAX]. (Without the − 0.57 per mil correction to WAX-1, the average value would have been + 0.97 ± 0.32 per mil.) In work with gaseous fuels, to be published elsewhere, using underventilated combustion (Léonard et al., 1994), we again found a tendency toward ^{13}C enrichment in the flaming aerosol from hydrocarbon fuel, with an even larger effect than for the solid hydrocarbon fuel.

4.3.4. Polycyclic aromatic hydrocarbons

Smoldering and flaming stage aerosols were assayed also for PAH, using supercritical fluid extraction (SFE) GC/MS with CO_2 as the working fluid. This method has the merit of treating quite small samples with little or no

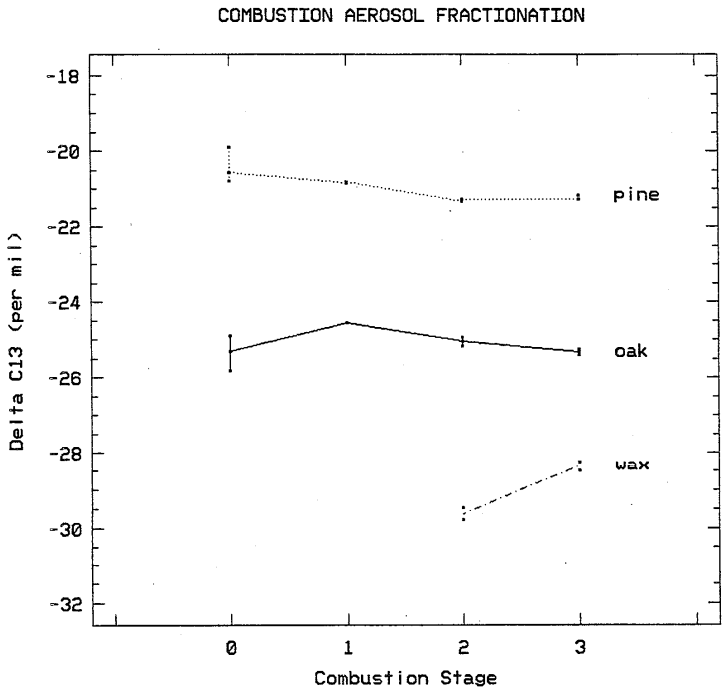

Fig. 6. Combustion aerosol isotopic fractionation. $\delta^{13}C$ values vs. combustion stage are given for three solid fuels (two woods, one hydrocarbon). Stage-0 represents the raw, heterogeneous pine and oak samples; stage-1 represents the homogenized wood reference samples; stages-2 and -3 represent smoldering and flaming, respectively. Isotope effects as small as 0.1 per mil required stable isotope ratio measurements of extreme precision, and preparation of special isotopically homogenous wood (oak, pine) reference materials. Note that, except for the triplicate raw wood samples, all data shown represent duplicate samples. The datum for the higher (more enriched) stage-2 wax sample has been adjusted downward by − 0.57 per mil, as explained in the text.

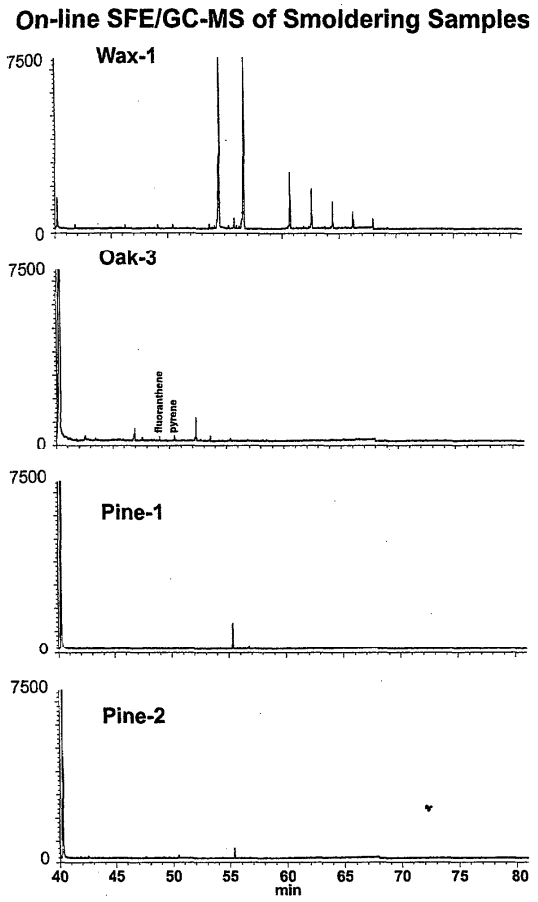

Fig. 7. Reconstructed ion chromatograms for the smoldering stage aerosols (ion abundance vs. retention time).

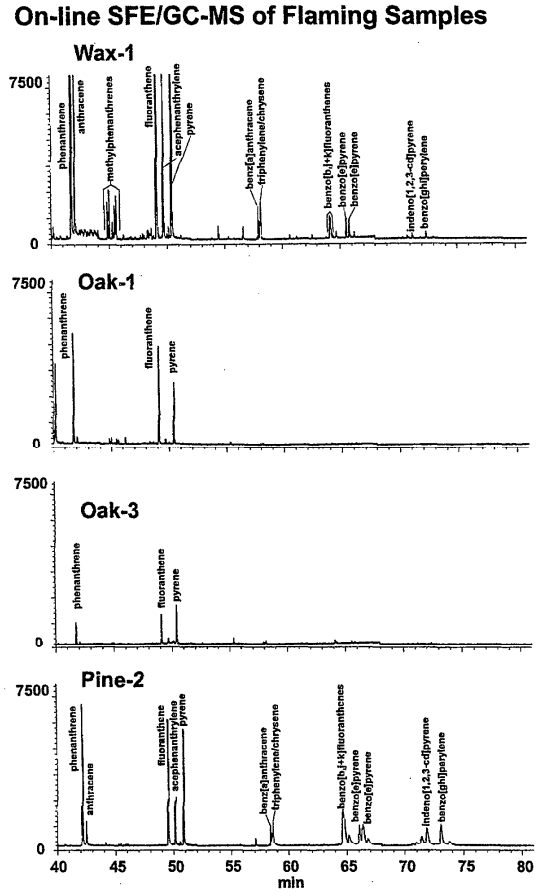

Fig. 8. Reconstructed ion chromatograms for the flaming stage aerosols (ion abundance vs. retention time).

sample handling. It has the capability of measuring $10\,\mu g\,g^{-1}$ levels of individual PAH in 100 μg aerosol filter samples (Madrzykowski and Stroup, 1998). Single ion monitoring (SIM) reconstructed ion chromatograms for smoldering stage aerosol samples are shown in Fig. 7, and flaming stage samples, in Fig. 8. The ions monitored were selected to cover PAH ranging from phenanthrene ($m = 178$ Da) to benzo(*ghi*)perylene ($m = 276$ Da). PAH above a critical peak height level of 250 (ordinate units) are appropriately labeled in Fig. 8 (flaming stage). Certain PAH occurred also in the smoldering aerosol samples, but their abundances were very much smaller, less than 1% of the largest levels in Fig. 7. The only PAH found in all samples analyzed were fluoranthene and pyrene.

The larger peaks in Fig. 7, therefore, were not PAH. Although unique identification has yet to be made, the series of peaks appearing in the smoldering stage chromatogram for paraffin wax-1 are suggestive of an electron impact fragmentation pattern for a normal alkane of mass greater than 252 Da. (The typical range for paraffin wax is 282 to 338 Da.) Thus, it seems reasonable that the very small amount of carbon, collected during the smoldering stage from the paraffin wax, results from distillation, perhaps with some cracking, of the source fuel, per se. The most obvious conclusion to be drawn from the flaming stage aerosol chromatograms is that paraffin wax and pine yield a full range of PAH, whereas oak shows little or nothing beyond pyrene.

In light of the earlier discussion of PAH in the Albuquerque atmosphere, there is a dual surprise. First, there is the absence of retene and esters of dehydroabietic acid in the laboratory combustion aerosol. In field studies where wood fuel includes conifers, such as the Albuquerque study (Sheffield et al., 1994) and a similar one in Denver (Klinedinst et al., 1997), the

occurrence of these substances is the rule. Clearly more samples must be processed to confirm these laboratory-field differences, but there is now independent evidence suggesting that the state of the sample (here, pine) may be quite influential in the thermal production of the conifer dehydrogenation products. (See Section 4.3.6.)

The second surprise relates to the heavier PAH, such as benzo(*ghi*)perylene. The results discussed in the first two parts of this paper suggested that such compounds in ambient urban atmospheres derive primarily from fossil fuel sources. The PAH data given here are consistent with that, if paraffin wax is a suitable surrogate for the urban fossil sources, and oak, for the urban biomass sources. The surprise was that pine, in its flaming mode, also produced the heavier PAH. That is not true, however, for the smoldering stage, where pine yielded quite a large ratio of carbon to our model PAH, pyrene. Using the pine and paraffin wax data in Table 2, we may set bounds for the relative amount of our surrogate PAH pyrene from biomass and fossil sources. For one extreme we assume that the biomass aerosol carbon comes totally from the smoldering stage, and the fossil carbon, from the flaming stage; the other extreme would take flaming stage carbon for both sources. The results, for equal contributions of fossil and biomass sources to the total aerosol carbon, for example, would be 94% fossil pyrene in the first case, and 58% in the second. These estimates, which are offered strictly for the sake of illustration, suggest that the observation of heavier PAH from the laboratory study is not necessarily discordant with the field data. They point, however, to the importance of further, and more directed experiments in both regimes.

4.3.5. A possible link between isotopic and molecular fractionation

Since both ^{13}C and PAH data are available as a function of fuel and stage of combustion, and both may reflect the impact of incomplete combustion, it becomes interesting to seek possible links between isotopic and molecular fractionation. Under the best of circumstances, an isotopic shift might serve as an index for a shift in a multivariate molecular source profile. That, in turn, could lead to improved accuracy in molecular marker source apportionment. It is interesting also to look for a possible relationship between the PAH data from the laboratory combustion study with the more extensive distribution of such data from the Albuquerque field study. Since pinyon pine was the principal biomass fuel in use in Albuquerque, we shall compare data for that fuel in the laboratory study. Since only two PAH, fluoranthene and pyrene, were observed in all aerosol samples examined, we shall use the relative PAH abundance, RPA = fluoranthene/(fluoranthene + pyrene), as the PAH metric. For the laboratory data for pine (smoldering, flaming) there was a positive correlation between $\delta^{13}C$ and RPA, but with only three samples the estimated correlation coefficient (0.85) can be considered suggestive, but certainly not statistically significant. The relationship between RPA in the laboratory and the field is, perhaps, a bit stronger. The entire picture is captured in Fig. 9.

The figure represents a superposition of the distribution of RPA values for ambient aerosol samples collected in Albuquerque (abscissa, right ordinate), and the $\delta^{13}C$ and RPA values for the smolder (Ps) and flaming (Pf) stage laboratory pine aerosol samples. Apart from the hint of a correlation between $\delta^{13}C$ and RPA for the three pine aerosol samples, the figure shows that the Ps and Pf PAH abundances lie, respectively, near the lower and upper ends of the Albuquerque RPA distribution. In particular, the Ps samples are close to a rather marked peak in the lower portion of that distribution. What makes this interesting is that the two smoldering aerosol samples (Ps) are in the region of the RPA distribution populated primarily by nighttime Albuquerque samples, whereas the flaming stage sample (Pf) is in the RPA region favored by the daytime field samples. The nighttime field samples and the smoldering stage laboratory samples had also something else in common: both had an excess of carbon compared to high temperature combustion aerosol components – as seen by the C/pyrene ratios in Table 2, and by the excess biomass carbon, compared to that predicted by the K–Pb multiple regression model in Currie et al. (1994), and shown in Fig. 1.

The above comments are offered in the spirit of a hint or conjecture, inspired by multivariate data arising in different contexts. Confirmatory experiments, including a suitable number of observations, are clearly needed. If these suggestions turn out to be valid, however, it could lead to a better understanding of the physics and chemistry of carbonaceous aerosol production in the laboratory and the ambient atmosphere, and it might provide an opportunity to utilize stable isotope data to 'sharpen' molecular marker profiles for improved identification and quantification of combustion aerosol sources.

4.3.6. The retene surprise

It is noteworthy that in the laboratory combustion study, in contrast to field studies, conifer thermal decomposition products of abietic and pimaric acids – namely, 1-methyl, 7-isopropyl phenanthrene [retene] and 1,7-dimethyl phenanthrene, and their dehydrogenation precursors – were *not* observed. Recent work at NIST (Madrzykowski and Stroup, 1998), however, may give some insight into this matter. The research in question was directed at examining the chemical products associated with fire extinguishing. When a pine 'crib' was burned under laboratory conditions, the result was similar to our results with the cone calorimeter: absence of the conifer dehydrogenation products. However, once the flame was extinguished with water, retene and methyldehydroabietate were produced in large

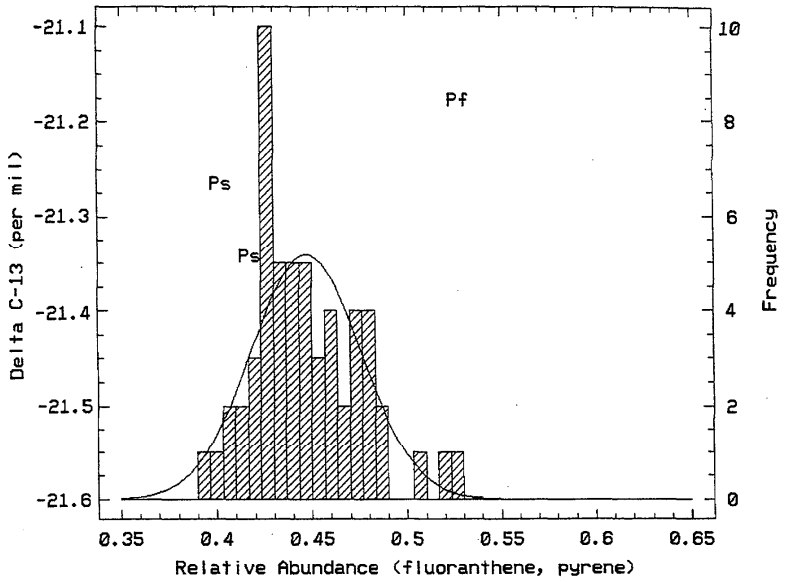

Fig. 9. Isotopic-chemical fractionation. Superposition of pine laboratory combustion aerosol (smolder: Ps, flame: Pf) isotopic composition [left ordinate, $\delta^{13}C$ (per mil)], and Albuquerque ambient aerosol PAH frequency distribution [right ordinate] vs. relative (fluoranthene, pyrene) PAH abundance (RPA) [abscissa]. There is a suggested correlation between $\delta^{13}C$ and RPA for the laboratory samples, with the Ps aerosol linked with the Albuquerque nighttime aerosol peak at ca. RPA = 0.43.

abundance. We are forced to recognize the effects, in the actual environmental setting, of not only fuel type and combustion stage, but of the conditions surrounding the combustion process. The presence of moisture and accompanying thermal effects, and even the close proximity of source material in different stages of combustion, may profoundly influence the nature and distribution of aerosol products.

5. Synthesis

There are many lessons to be learned from the synthesis of results from these investigations of carbon isotopes and combustion aerosol, from three different perspectives. The most important, perhaps, is that each approach brings new light regarding the nature of the process, including some very important independent confirmation, but also introducing new insights or at least observations of unsuspected behavior. Consideration of the prior, published investigations (Albuquerque field study, GC/AMS characterization of the atmospheric aerosol reference material), by themselves, and in light of the new work (laboratory combustion study), leads to the following highlights.

- The mixed biomass-fossil urban carbonaceous aerosol could not be described adequately by the K, Pb elemental tracer model, especially at night. Isotopic data (^{14}C) pointed to the presence of excess biomass soot carbon at night, accompanied by significant amounts of conifer dehydrogenation products (retene, methyldehydroabietate). The correlation between Pb and benzo(*ghi*)perylene pointed to a largely fossil origin for this heavy PAH.
- The urban particle reference material, SRM 1649a, provided a special opportunity to examine isotopic heterogeneity in carbonaceous aerosol at the molecular level. The relative abundance of combustion products of different (fossil, biomass) sources was reflected dramatically in the ^{14}C composition, ranging from essentially pure fossil from the aliphatic fraction to only about half of that for the total carbon. The result for benzo(*ghi*)perylene was consistent with the multivariate statistical implication (largely fossil), but the rather precise AMS data was degraded a bit by the presence of an unresolved complex mixture (*ucm*) accompanying the PAH peak. The off-line GC/AMS technique offers great promise for the study of carbonaceous material in the atmosphere at the molecular level, and it provides the chance to derive source profiles at the receptor (sampling) site, by direct isotopic assay, as opposed to indirect, multivariate techniques that often lack unique solutions in the absence of unproven assumptions.

- The initial stable (^{13}C) isotopic compositions of the deciduous and conifer wood fuels used in the laboratory combustion study, point up the fact that plants deriving from the same photosynthetic mechanism (C3) can nevertheless be sufficiently different that, other things being equal, ^{13}C alone could quantitatively apportion carbonaceous aerosol representing two-component mixtures of such sources. That would make the application of dual isotopic (^{13}C, ^{14}C) characterization of individual chemical fractions even more interesting, but first the possibility of combustion-induced isotopic fractionation must be considered. The laboratory study showed that measurable isotopic fractionation did occur, ranging from ca. -0.7 per mil to $+1.3$ per mil for the solid fuels studied, with a change in sign in passing from the wood fuels to the hydrocarbon fuel. Fractionation of this magnitude already limits any simplistic application of ^{13}C to within-class (e.g., C3) apportionment. It also means that precise isotope measurements are essential to determine such fractionation effects, and, for isotopically heterogeneous fuels such as the woods, preparation of homogeneous, source reference materials is mandatory. The isotopically homogeneous wood specimens produced for this project are believed to be the first such reference materials.
- The dramatic dependence of elemental and organic aerosol carbon and PAH production on fuel type and combustion stage showed that the effects of both of these factors must be taken into account in field studies, and it lends support to the idea that the excess biomass carbon observed in the nighttime Albuquerque samples may be related to the predominance of the smoldering stage. This would support also the greater association of PAH with fossil carbon, since there was essentially no smoldering stage for the hydrocarbon fuel. Confounding of these factors (fuel type, combustion conditions) leads to difficulties in using EC/TC for fossil/biomass aerosol apportionment, so it becomes increasingly important to develop effective EC isolation procedures for the direct ^{14}C apportionment of this component, as described in our companion paper on remote carbonaceous aerosols (Currie et al., 1998b).
- The near absence of a 'glow' (char) stage for the hydrocarbon fuel, in contrast with the wood fuels is directly analogous to the charring issue in thermal approaches for the isolation of EC for isotopic measurement. The large production of char from the woods (ca. 20% of the initial mass), but not from the hydrocarbon fuel, is similar to the char production determined by the thermal-optical method of determining EC in SRM 1649a, where charring has been shown to approximately double the apparent EC (R. Cary, personal communication, 1998).
- Two interesting outcomes or surprises from the laboratory study were: (1) the production of heavy PAH from pine, yet its absence from oak, and (2) the 'retene surprise'. Production of heavy PAH from pine is not necessarily inconsistent with the statistical result from the Albuquerque experiment or the direct ^{14}C – PAH characterization results of the GC/AMS experiment, because of the 'diluting' effect of non-PAH carbonaceous aerosol produced during the smoldering stage. The 'retene surprise' highlights the importance of fuel or combustion conditions on the chemical products of combustion. It means that extreme caution is needed in trying to apply a linear (conservative) tracer model to apportion sources of organic combustion aerosol under field conditions.[3]

6. Outlook and conclusion

Much work remains to be done. For the GC/AMS technique to attain an optimal level of application, problems associated with '*ucm*' or chromatographic peaks that do not reach baseline-resolved purity must be solved. For materials such as the urban particle SRM, this has already been achieved using the special liquid chromatographic clean up procedures mentioned earlier. Refining the technique to permit on-line injection into an AMS ion source would be an important advance (Schneider et al., 1998), as would developments to limit or fix the ^{13}C isotopic fractionation that accompanies incomplete trapping of chromatographic peaks. The GC/AMS results for SRM 1649a, incidentally, suggest a lack of isotopic-mass balance, at least for the chemical fractions listed in Table 1. It would be very interesting to investigate the isotopic composition of polymeric organic fractions, such as humic substances and cellulose, that have been reported recently in atmospheric aerosols (Havers et al., 1997; Twaroch and Puxbaum, 1997).

More extensive experimental research on the laboratory combustion process is needed to complement the work reported here. A first step will be to extend the research to include C4 plant material, so important to biomass burning in the tropics. Also, if enough material can be produced, molecular scale ^{13}C and ^{14}C aerosol data would be quite valuable (Currie et al., 1997; Norman et al., 1997); and certainly microparticle characterization, yields of trace elements, and yields and isotopic compositions of gaseous products (CO, CH_4) and of 'elemental

[3]We are in the process of obtaining comparative, carbon (isotopic and chemical) field data from a controlled-burn boreal crown fire (N.W.T., Canada) that was sampled in July 1998 (J.M. Conny, personal communication).

carbon' should be studied, as a function of fuel and combustion stage. Isotopic-chemical fractionation of gaseous hydrocarbon fuels, mentioned briefly in Section 4, should be further investigated. Much could be learned also by investigating carbon ion clusters and the remarkable sequence of PAH molecular ions that has been observed in diffusion flame soot particles (Dobbins et al., 1997). Finally, the conjecture of covariance between isotopic and chemical fractionation (Fig. 9) should be put to rest, or supported, by additional measurements. Much opportunity, and need, exists for a basic theoretical understanding of the isotopic-chemical changes observed here. We do not presume to have made serious inquiries into the body of knowledge that may exist in this area, but it seems clear that an initial step would be to design laboratory combustion experiments with pure substances, before attempting to develop a fundamental understanding of something so complex as wood. The latter, however, is a major player in biomass burning, especially in the sensitive boreal regions, so it is nevertheless appropriate to continue to build empirical understanding of these complex systems.

To end on a cautious note: the effects of combustion stage on elemental and organic aerosol products, of combustion-induced isotopic fractionation, and the effects of combustion conditions on dehydrogenation products, suggest that a certain amount of circumspection is in order in the application of presumed conservative elemental or organic tracers to so complicated a system. The use of two or more independent approaches, as illustrated here, is clearly one of the best means to avoid the pitfalls associated with erroneous model assumptions.

Note added in proof. Important new work on baseline resolved PAH, mentioned at the end of Section 3.3, has resulted in a ^{14}C value for benzo[*ghi*]perylene, free from *ucm* interference. That is 8.6 ± 0.5 percent modern, which, when adjusted for atmospheric nuclear testing, is equivalent to 93.9 ± 0.4 percent fossil carbon. While consistent with the previous conclusion that this compound in SRM 1649a derives predominantly from fossil fuel combustion, the greatly decreased (standard) uncertainty indicates a minor but definite biomass carbon component of ca. 6 percent, consistent with a small contribution from a biomass fuel such as pine wood. By applying isotopic mass balance to the combined new (baseline resolved) and old (*ucm* containing) data, we can also derive an estimate for the *ucm* ^{14}C. That is 21 ± 1 percent modern, or 85 ± 1 percent fossil carbon, comparable to the average composition of the aromatic fraction of SRM 1649a as given in Table 1.

Acknowledgements

We gratefully acknowledge contributions from the following individuals: T. Coplen and J. Hopple, for ^{13}C measurements; and J.M. Conny, J. Lee, G.W. Mulholland, and B.J. Porter, for advice and/or assistance with laboratory combustion experiments. Partial support for the research was provided by NASA Grant Number W-18959.

References

Babrauskas, V., 1982. Development of the cone calorimeter—a bench-scale heat release apparatus based on oxygen consumption. National Bureau of Standards NBSIR 82–2611.

Buffle, J., Van Leeuwen, H.P. (eds.), 1992. Environmental Particles, IUPAC Environmental Analytical Chemistry Series, vol. I. Lewis Publishers, Boca Raton, FL.

Cachier, H., 1989. Isotopic characterization of carbonaceous aerosols. Aerosol Science and Technology 10, 379–385.

Cachier, H., Pertuisot, M-H., Liousse, C., Delmas, R., Jaffrezzo, J-L., Legrand, M., Wolff, E., 1997. Combustion particles in the polar atmosphere, this Conference, Paper P3.

Coplen, T.B., De Bièvre, Krouse, H.R., Vocke, R.D., Jr., Grönig, M., Rosanski, K., 1996. Guidelines for reporting stable H, C, and O isotope-ratio data. EOS, Transactions, American Geophysical Union 77, [27] 255.

Currie, L.A., Klouda, G.A., Voorhees, K.J., 1984. Atmospheric carbon: the importance of accelerator mass spectrometry. Nuclear Instruments and Methods 233, 371–379.

Currie, L.A., Sheffield A.E., Riederer, G.E., Gordon, G.E., 1994. Improved atmospheric understanding through exploratory data analysis and complementary modeling: the urban K-Pb-C system. Atmospheric Environment 28, 1359–1369.

Currie, L.A., Eglinton, T.I., Benner, Jr., B.A., Pearson, A., 1997. Radiocarbon 'dating' of individual chemical compounds in atmospheric aerosol: first results comparing direct isotopic and multivariate statistical apportionment of specific polycyclic aromatic hydrocarbons, Nuclear Instruments and Methods Physics Research 123, 475–486.

Currie, L.A., Dibb, J.E., Klouda, G.A., Benner, Jr, B.A., Conny, J.M., Biegalski, S.R., Klinedinst, D.B., Cahoon, D.R., Hsu, N.C., 1998a. The pursuit of isotopic and molecular fire tracers in the polar atmosphere and cryosphere. Radiocarbon 40, 381–390.

Currie, L.A., Dibb, J.E., Klouda, G.A., Slater, J., Biegalski, S.R., Benner, Jr., B.A., Biddulph, D., 1998b. Remote atmospheric and glacial records of biomass burning. This Conference, Paper O11.

Dobbins, R.A., Fletcher, R.A., Chang, H.-C., 1997. The evolution of soot precursor particles in a diffusion flame. Combustion and Flame 115, 285–298.

Eglinton, T.I., Aluwihare, L.I., Bauer, J.E., Druffel, E.R.M., McNichol, A.P., 1996. Gas chromatographic isolation of individual compounds from complex matrices for radiocarbon dating. Analytical Chemistry 68, 904–912.

Friedlander, S.K., 1973. Chemical element balances and identification of air pollution sources. Environmental Science and Technology 7, 235–240.

Fritz, P., Fontes, J.Ch. (eds.), 1980. Handbook of Environmental Isotope Geochemistry, vol. 1. Elsevier, Amsterdam.

Goldberg, E.D., 1985. Black Carbon in the Environment. Wiley-Interscience, New York, NY.

Gordon. G., 1988. Receptor models. Environmental Science and Technology 22, 1132–1142.

Havers, N., Burba, P., Klockow, D., 1997. Characterization of humic-like substances in airborne particulate. This Conference, Paper O22.

Hopke, P.K., 1985. Receptor Modeling in Environmental Chemistry. Wiley, New York.

Klinedinst, D.B., Kenniston, G.E., Benner, Jr, B.A., Klouda, G.A., 1997. Evaluation of the residential woodburning contribution to PM_{10} carbon in Denver, Colorado using radiocarbon analysis. Environmental Science and Technology (submitted).

LaFlamme, R.E., Hites, R.A., 1978. The global distribution of polycyclic aromatic hydrocarbons in recent sediments. Geochimica et Cosmochimica Acta 42, 289–300.

Lèonard, S., Mulholland, G.W., Puri, R., Santoro, R.J., 1994. Generation of CO and smoke during underventilated combustion. Combustion and Flame 98, 20–34.

Lewis, C.W., Einfeld, W., 1985. Origins of carbonaceous aerosol in Denver and Albuquerque during winter. Environment International 11, 243–247.

Madrzykowski, D., Stroup, D.W., (Eds.), 1998. Demonstration of Biodegradable, Environmentally-Safe Non-toxic Fire Suppression Liquids, Ch. 4. NIST Special Report 6191.

Masclet, P., Hoyau, V., 1994. Evidence for the presence of polycyclic aromatic hydrocarbons in the polar atmosphere and in polar ice. Analusis 22, M31–M33.

NIST Certificate of Analysis for Standard Reference Material 1649, Urban Dust/Organics (Apr. 1982; Jan. 1992). Recertification data for SRM 1649a, 1998. In: Wise, S.A., Schantz, M.M., Hays, M.J., Koster, B.J., Sharpless, K.E., Sander, L.C., Benner Jr, B.A., Schiller, S.B., 1996. Certification of PAHs in mussel tissue and air Particulate SRMs. Journal of Polycyclic Aromatic Compounds 9, 209–216.

Norman, A.L., Blanchard, P., Hopper, J.F., Ernst, D., 1997. Stable carbon isotope composition of atmospheric PAHs and n-alkanes. This Conference, Paper O27.

Pearson, A., Eglinton, T.I., McNichol, A.P., Currie, L.A., Schneider, R.J., von Reden, K.F., Benner, Jr, B.A., Wise, S.A., 1997. Determination of the radiocarbon ages of individual PAH extracted from urban aerosol and marine sediment. International Radiocarbon Conference, paper 148, Groningen.

Penner, J.E., Novakov, T., 1996. Carbonaceous particles in the atmosphere: a historical perspective to the Fifth International Conference on Carbonaceous Particles in the Atmosphere. Journal of Geophysical Research 101 (D14), 19,373–19,378.

Rogge, W.F., Mazurek, M.A., Hildemann, L.M., Cass, G.R., Simoneit, B.R.T., 1993. Quantification of urban organic aerosols at a molecular level: identification, abundance, and seasonal variation. Atmospheric Environment 27, 1309–1330.

Schneider, R.J., Hayes, J.M., Von Reden, K.F., McNichol, A.M., Eglinton, T.I., 1998. Target preparation for continuous flow accelerator mass spectrometry. Radiocarbon 40, 95–102.

Sheffield, A.E., Gordon, G.E., Currie, L.A., Riederer, G.E., 1994. Organic, elemental, and isotopic tracers of air pollution sources in Albuquerque, NM. Atmospheric Environment 28, 1371–1384.

Sturges, W.T., Barrie, L., 1987. Lead 206/207 ratios in the atmosphere of North America as tracers of US and Canadian emissions. Nature 329, 144–146.

Twaroch, A., Puxbaum, H., 1997. Cellulose in atmospheric aerosols and wet precipitation. This Conference, Paper P16.

Wise, S.A., Chesler, S.N., Hertz, H.S., Hilpert, L.R., May, W. E., 1977. Chemically-bonded aminosilane stationary phase for the high-performance liquid chromatographic separation of polynuclear aromatic hydrocarbons. Analytical Chemistry 49, 2306.

Zeisler, R., Langland, J.K., Harrison, S.H., 1983. Cryogenic homogenization of biological tissues. Analytical Chemistry 55, 2431–2434.